Korean J. Chem. Eng., 35(2), 489-497 (2018)
DOI: 10.1007/s11814-017-0321-9

pISSN: 0256-1115
eISSN: 1975-7220

Recovery of nitrate from water streams using amine-grafted and magnetized SBA-15

Seong Chul Ryu*, Ji Yoon Kim*, Min Jin Hwang, and Hee Moon*,†**

*School of Chemical Engineering, Chonnam National University, 77 Yongbong-ro, Gwangju 61186, Korea
**Department of Environmental System Engineering, Chonnam National University,
50 Daehak-ro, Yeosu, Jeonnam 59626, Korea
(*Received 20 September 2017 • accepted 20 November 2017*)

Abstract−Mesoporous silica SBA-15 was modified using amine-grafting and magnetization to enhance its nitrate adsorption capacity and to render the spent silica particles recoverable from the working solution after use. Such modifications result in an outstanding adsorbent for recovering nitrate from water streams by adding high adsorption ability and easy handling to the intrinsic properties of SBA-15. When the molar ratio of SBA-15 to 3-aminopropyltriethoxysilane (APTES) is 10 : 3 during amine-grafting, the resulting SBA-15G-4 sample exhibits the highest nitrate adsorption capacity (44.9 mg/g) among the tested materials. The other sample, 67-SBA-15MG, which was magnetized with iron nitrate content of 67 wt% of SBA-15, exhibits sufficient magnetic force for recovery from the working solution, while maintaining ~81% of nitrate adsorption capacity of the corresponding amine-grafted SBA-15G-5. Furthermore, the 67-SBA-15MG material retains its adsorption capacity and magnetic strength after ten adsorption/desorption cycles, indicating excellent characteristics as a magnetically recyclable adsorbent for recovering nitrate.

Keywords: Recovery of Nitrate, SBA-15, Amine-grafting, Magnetization, Recyclable Adsorbent

INTRODUCTION

Water is the most important resource for life on earth, yet only ~2.66% of water resources on earth are suitable for human use and only 0.6% is available as drinking water [1]. Therefore, it has become vital to treat domestic sewage, industrial effluents, and agriculture effluents in order to secure water resources. The removal and recovery of nitrate from wastewater is especially important for human health and the environment [2]. Although nitrification can prolong water exchange in aquaculture tanks, high nitrate concentrations nevertheless cause eutrophication and health problems, such as blue-baby syndrome and stomach cancer [3,4]. Therefore, the effective recovery of nitrate from wastewater streams serves two purposes by both purifying the water and providing nitrate that can be reused as fertilizer or as a raw chemical in industry [2]. To achieve this, reliable recycle processes must be devised which facilitate the recovery of valuable nutrients such as nitrate. Presently, several treatment processes for nitrate recovery have been devised, such as ion exchange, reverse osmosis, electro-dialysis, biological treatment, and adsorption [5-7]. Among these, adsorption has been widely used because of its convenience, high efficiency, and low operating cost [8]. Conventional adsorbents such as chitosan, pumice, and activated carbon have been employed for removing nitrate from water [6-9]. However, in general, they fall short of expectations when applied in the field due to their low nitrate adsorption capacities.

Therefore, the preparation of high-quality adsorbents with high physical and chemical stabilities as well as high adsorption capacity is imperative. Mesoporous silica materials receive a great deal of attention as reliable adsorbents due to their large surface area, tunable porosity, uniform pore size, and high thermal stability [10]. Since M41S, the family of mesoporous silica which includes materials such as MCM-41, was discovered in 1992 [11], the synthesis of surfactant-template mesoporous silica materials under various conditions has been developed. Subsequently, another type of mesoporous silica, namely SBA-15, was synthesized in 1998 using triblock-copolymers [12]. This SBA family of mesoporous silica materials can be synthesized with large pore size and thicker pore walls. Furthermore, the pore sizes of SBA-15 series can be easily tuned to be between 2 nm to 30 nm by applying swelling agents such as trimethylbenzene (TMB) [12,13]. In the synthesis of SBA-15, the triblock copolymer surfactants used as structure-directing agents (SDA) can form micelles in certain concentrations [14], resulting in hexagonal, lamellar, and cubic structures [15,16]. However, it is known that pristine SBA-15 does not have sufficient adsorption capacity for nitrate, despite of the many advantages mentioned above [17].

Chemical modification of SBA-15 can be undertaken to increase the number of active adsorption sites and enhance its nitrate adsorption capacity. Saad et al. [17] synthesized amino-functionalized mesoporous silica materials by co-condensation and post-synthesis grafting methods using APTES as an amine-functional group source. The results indicate that amine grafting is a promising method of increasing adsorption capacity. Subsequently, several researchers used similar techniques to enhance the adsorption capacity of mesoporous silica materials for metal and metal oxides [18-20]. Another important concern in many adsorption processes is to recover spent adsorbents effectively from working solutions for

†To whom correspondence should be addressed.
E-mail: hmoon@jnu.ac.kr

subsequent use. However, conventional recovery processes, such as filtration and centrifugation, are not always appropriate, especially when powder-type adsorbents are used. Furthermore, if the adsorbent is not completely recovered, it may cause secondary environmental contamination. Therefore, the magnetic separation of power-type spent adsorbents is highly desirable in many applications [21]. The preparation of magnetically separable mesoporous silica materials has been an active area of research [22-24]. Iron(III) nitrate has been used for magnetization to form mag-hematite, γ-Fe_2O_3, which not only has hematite characteristics but also exhibits its magnetic properties [24]. Kim et al. [21] synthesized magnetically separable SBA-15 by a post-synthesis method. They reported that after magnetization the adsorption capacity was slightly reduced. However, the spent adsorbents were successfully separated from the working solution by external magnetic force.

In this work, highly ordered mesoporous silica SBA-15 was hydrothermally prepared in a batch reactor and characterized by various methods. In addition, it was amine-grafted and magnetized to prepare a magnetically recyclable adsorbent for recovering nitrate from water streams. The modified adsorbents were carefully evaluated through equilibrium and batch adsorption tests.

EXPERIMENTAL

1. Materials and Preparation

Poly(ethylene glycol)-block-poly(propylene glycol)-block-poly (ethylene glycol) (P123) and tetraethyl orthosilicate (TEOS) (98%, Sigma-Aldrich) were used as a structure directing agent and a silica source. Hydrochloric acid (HCl, 37% Sigma-Aldrich), was diluted to make 2 M HCl acid solution. (3-Aminopropyl) triethoxysilane (APTES, Sigma-Aldrich) and dry toluene (99.8%, Sigma-Aldrich) were used for amine-grafting. $Fe(NO_3)_3{\cdot}9H_2O$ (≥98%, Sigma-Aldrich), methanol (99.8%, Sigma-Aldrich), and propionic acid (≥99.5%, Sigma-Aldrich) were used for magnetization of SBA-15. Potassium nitrate (KNO_3 ≥99.0%, Sigma-Aldrich), was used to prepare nitrate solutions. For the desorption step, sodium hydroxide (NaOH) (≥98%, Sigma-Aldrich) was used to prepare 0.01 M NaOH solution.

Mesoporous silica material, SBA-15, was synthesized by a hydrothermal reaction. 12.0 g of P123 was dissolved in 480 ml of 2 M HCl aqueous solution and 90 ml of deionized water (DI-water). Subsequently, 25.5 g of TEOS was added into the solution which was stirred for 5 min at room temperature. The mixture was transferred to a polypropylene bottle and the hydrothermal reaction was carried out. The bottle was kept at 35 °C for 20 h and subsequently at 100 °C for one day. Finally, the product was filtered and then dried at 80 °C for 24 h. The final white powder product was calcined at 550 °C at a rate 4.5 °C/min for 3 h in air to remove the surfactant P123 from the product.

2. Modification of Adsorbents

SBA-15 is a silica material with bonded Si and OH groups. APTES is an amine source which has three ethyl groups and one amine functional group. The three OH groups on the SBA-15 may connect to the silica group on the APTES through bond formation at high temperatures, releasing ethanol. In amine-grafting, SBA-15 was modified employing the post-grafting method suggested by Saad et al. [17]. Solutions containing 16 mmol of SBA-15 powder were mixed with APTES to obtain solutions containing varying APTES concentrations (0.8, 1.6, 3.2, 4.8, 6.4 and 8.0 mmol) in dry toluene. The mixtures were refluxed and stirred at 110 °C for 10 h. The product was filtered, washed with isopropyl alcohol (IPA), and subsequently dried at room temperature for a day. Thereafter, acidification was undertaken using 0.1 M HCl solution at room temperature for 6 h. Finally, the amine-grafted mesoporous silica SBA-15 (SBA-15G series) was obtained.

Iron ore comes in two forms: magnetite (Fe_3O_4) and hematite (Fe_2O_3). Magnetite is a black magnetic iron material, whereas hematite is a red non-magnetic material. There are two types of hematite: α-hematite and γ-hematite [23,24]. The material of interest in this work is γ-hematite, which exhibits both hematite properties and magnetic force. In this work, iron nitrate was converted to γ-hematite using propionic acid. Small γ-hematite powder particles were formed on the surface of the SBA-15. Various amounts of iron nitrate (0.67, 1.01, 1.34 g) were dissolved in methanol and 0.5 g of SBA-15 was dispersed for magnetization. The mixture was dried at 80 °C for 12 h. The powder was treated with propionic acid vapor at 105 °C for 10 h. The final product was oxidized at 300 °C in air for 30 min at a rate of 1 °C/min. Finally, the magnetized SBA-15MG samples were obtained by amine-grafting as described above.

3. Characterization of Adsorbents

X-ray diffraction (XRD) was used to determine the structures of SBA-15 materials. All XRD patterns were recorded with a high-resolution X-ray diffractometer (X'Pert PRO Multi-Purpose X-Ray Diffractometer) using a Cu-Kα radiation source in a 2θ range of between 0 and 10° at a scan speed of 2°/min, at 40 kV and 20 mA. The physical properties of all samples were characterized by nitrogen isotherm data measured at 77 K using a BELsorp mini II adsorption analyzer (SOLETECK). The surface area and pore size distribution were evaluated by Brunauer-Emmett-Teller (BET) and Barrett-Joyner-Halenda (BJH) methods. Fourier transform infrared (FT-IR) spectra of all samples were obtained using an FT-IR-410 spectrometer (Jasco). The surface morphology of all the samples was also investigated using a JEM-2100F (JEOL) field-emission transmission electron microscope (FE-TEM) at 200 kV.

4. Removal of Nitrate

Adsorption of nitrate on the prepared adsorbents was investigated in a batch system. For this experiment, 0.1 g of adsorbent sample and 50 ml of nitrate solution were added into each bottle. The nitrate solutions were made from potassium nitrate (KNO_3). The bottles were kept in a shaking incubator at 20 °C with agitation at 200 rpm for 24 h to allow the samples to reach equilibrium. The initial concentrations of nitrate were in the range of 10 to 300 mg/L (ppm). The concentrations of nitrate in treated solutions were determined using a UV-spectrometer (UV-1601, SHIMADZU).

To investigate reusability of the amine-grafted magnetized SBA-15 (SBA-15MG), adsorption and desorption experiments were undertaken over ten cycles. After adsorption experiments, spent silica powder was magnetically removed from the working solution. Subsequently, the removed powder was mixed with 0.01 M NaOH solution to recover the nitrate. Basic solutions can bring

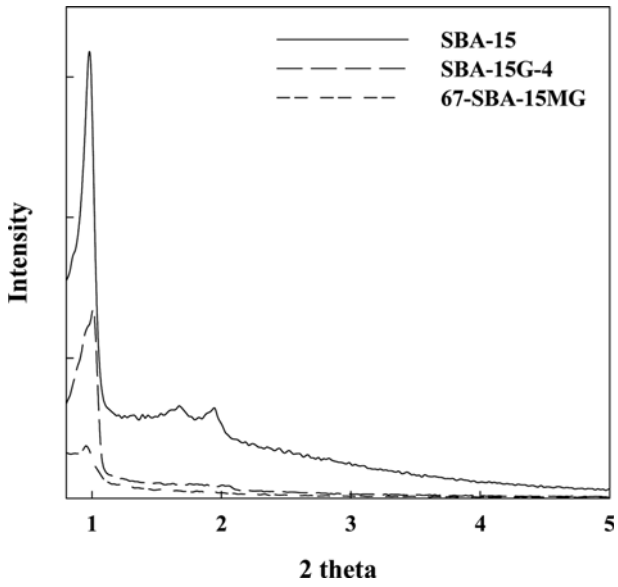

Fig. 1. XRD patterns of three selected samples.

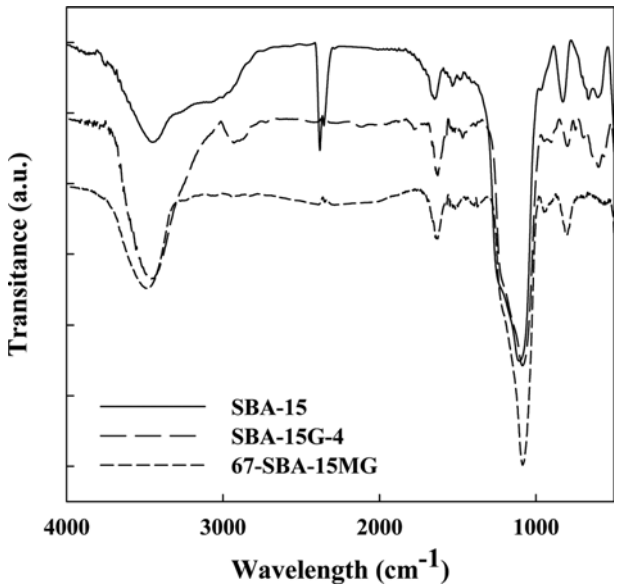

Fig. 2. FT-IR spectra of three selected samples.

about nitrate desorption by deprotonation of the acidified amine-groups (NH_3^+) to give the group in the neutral charge state (NH_2). The recovered silica powder was filtered, washed with DI-water, and dried at 80 °C. The recovered adsorbents must be acidified prior to use. Hence, the dried powder was mixed with 0.1 M HCl solution for 6 h. The regenerated adsorbent was used for further the batch adsorption experiments.

RESULTS AND DISCUSSION

1. Characterization Results

X-ray diffraction patterns of SBA-15, SBA-15G-4, and 67-SBA-15MG samples are shown in Fig. 1. The XRD pattern of mesoporous silica, SBA-15, shows three peaks at low angles in the 2θ range of 0-10°. Three peaks typical for the pristine SBA-15, one high intensity peak (100), and two small peaks (110) and (200), are observed. In separate analyses (not shown), the (100) peak was seen to become sharper and another two peaks clearly appeared, after aging for 20 h at 35 °C. This implies that the mixture can grow into a hexagonal structure even at 35 °C. This product would be expected to be stronger and more durable during high temperature reaction at 100 °C for a sufficient period.

After amine-grafting to the pristine SBA-15, the (100) peak significantly decreases and the two small peaks gradually disappear, as seen from the XRD pattern of the SBA-15G-4 material shown in Fig. 1. This indicates that the modification of the mesoporous silica (SBA-15) appears to result in severe blocking of pores. However, it does not affect the skeletal structure of mesoporous silica since the modification does not disrupt the structure physically. This point will be discussed again later in the context of the TEM and BET results. Furthermore, after magnetization of the particles using γ-hematite, the (100) peak almost completely disappears, as seen in the XRD pattern of the 67-SBA-15MG material. This can be attributed to the blocking effect of γ-hematite formed on the surface of the mesoporous silica.

FT-IR spectra of SBA-15, SBA-15G-4, and 67-SBA-15MG samples are shown in Fig. 2. Some variations in the spectrum of the SBA-15G-4 were observed after grafting, especially for the peaks assigned to amine-related groups. The broad peak at 3,500-3,100 cm^{-1} becomes more prominent after grafting. This peak is assigned to the N-H stretching. Furthermore, a peak at 1,350-1,000 cm^{-1}, which assigned to the N-H bonding, is seen to become sharp. Moreover, the small peak at 1,640-1,550 cm^{-1} becomes slightly larger after grafting. The observations pertaining to these three peaks indicate that amine-grafting on the SBA-15 is successful. However, no significant change is observed upon magnetization in the spectrum of the 67-SBA-15MG material, as expected. Magne-

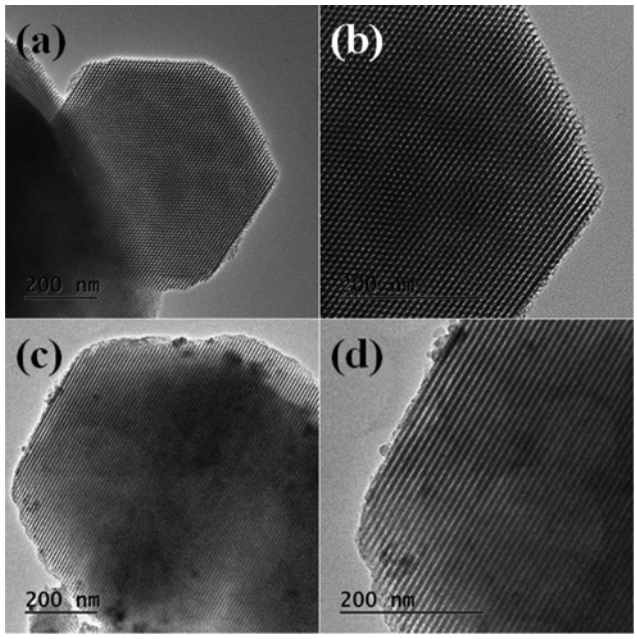

Fig. 3. TEM images. (a) and (b): SBA-15, (c) and (d): 67-SBA-15MG.

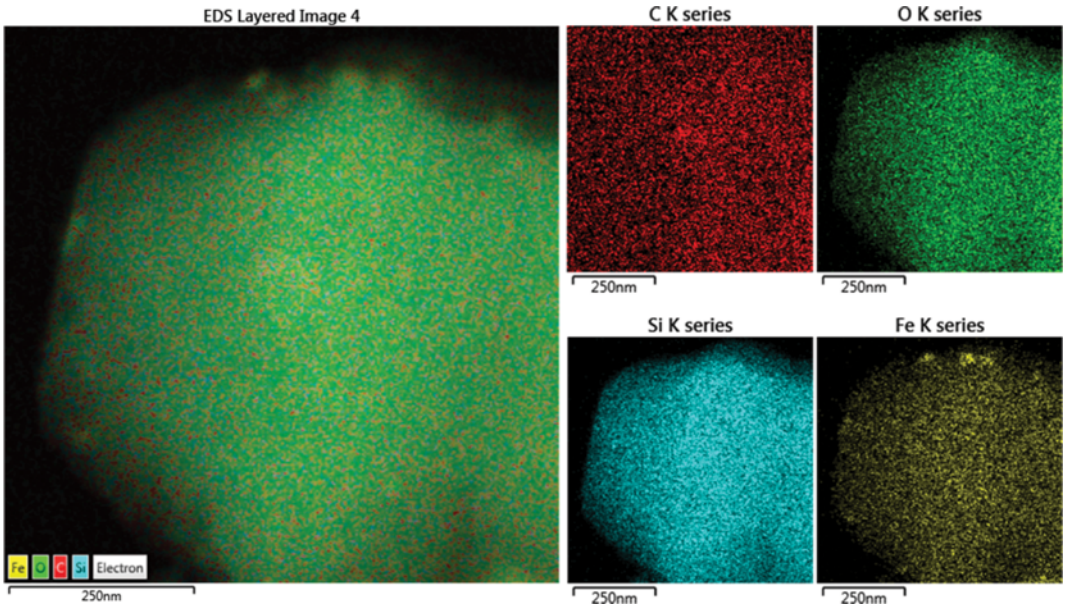

Fig. 4. EDS results for 67-SBA-15MG.

Table 1. EDS results for amine-grafted and magnetized 67-SBA-15MG

Element	Wt%	Atomic%
O	34.0	50.3
Si	51.9	43.7
Fe	14.2	6.01
Total	100	100

Fig. 5. Magnetic separation of 67-SBA-15MG powder.

tization appears to be a kind of doping of γ-hematite that introduces magnetism on the external surface but does not affect the surface functional groups formed inside pores [17].

TEM images of SBA-15 and 67-SBA-15MG are shown in Fig. 3. Figs. 3(a) and (b) are images of the pristine SBA-15 and show a clear two-dimensional (2D)-hexagonal and well-ordered mesoporous structure. Hence, it has been demonstrated that highly

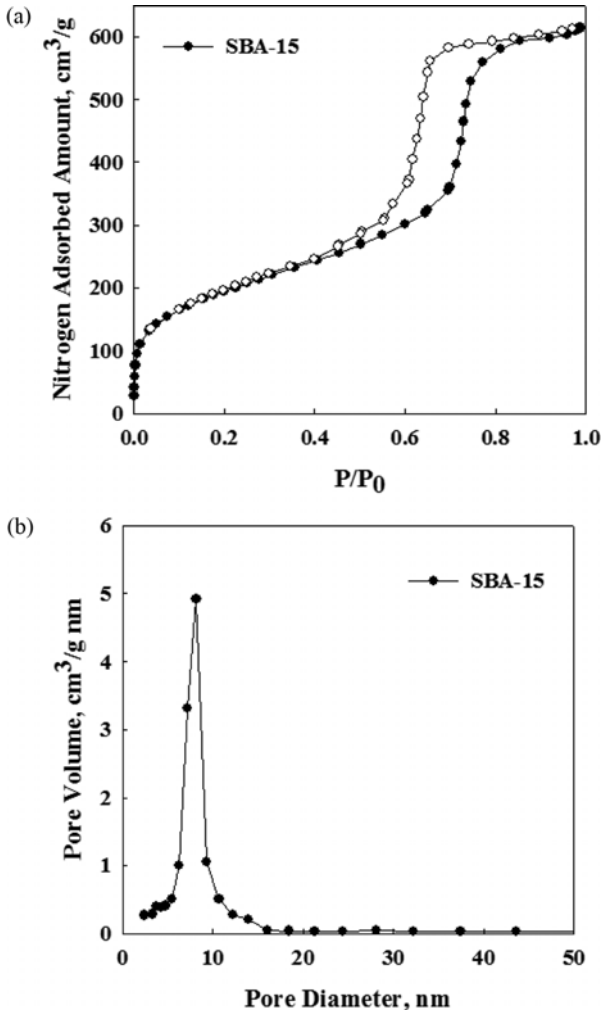

Fig. 6. (a) Nitrogen adsorption and desorption curves, (b) BJH pore size distribution of pristine SBA-15.

Table 2. Textural properties of pristine SBA-15 and amine-grafted SBA-15G series materials

Adsorbents	BET surface area	Total pore volume	BJH peak position	Amine loaded	Adsorption amount of nitrate*
	m^2/g	cm^3/g	nm	g	mg/g
SBA-15	699	0.86	8.19	0.000	2.86
SBA-15G-1	475	0.68	7.18	0.027	12.5
SBA-15G-2	390	0.56	6.30	0.173	27.4
SBA-15G-3	266	0.41	6.30	0.319	37.9
SBA-15G-4	223	0.35	6.30	0.376	44.9
SBA-15G-5	225	0.34	6.30	0.378	42.1
SBA-15G-6	192	0.30	6.30	0.362	37.7

*Adsorption amounts at equilibrium using initial concentration of 300 mg/L

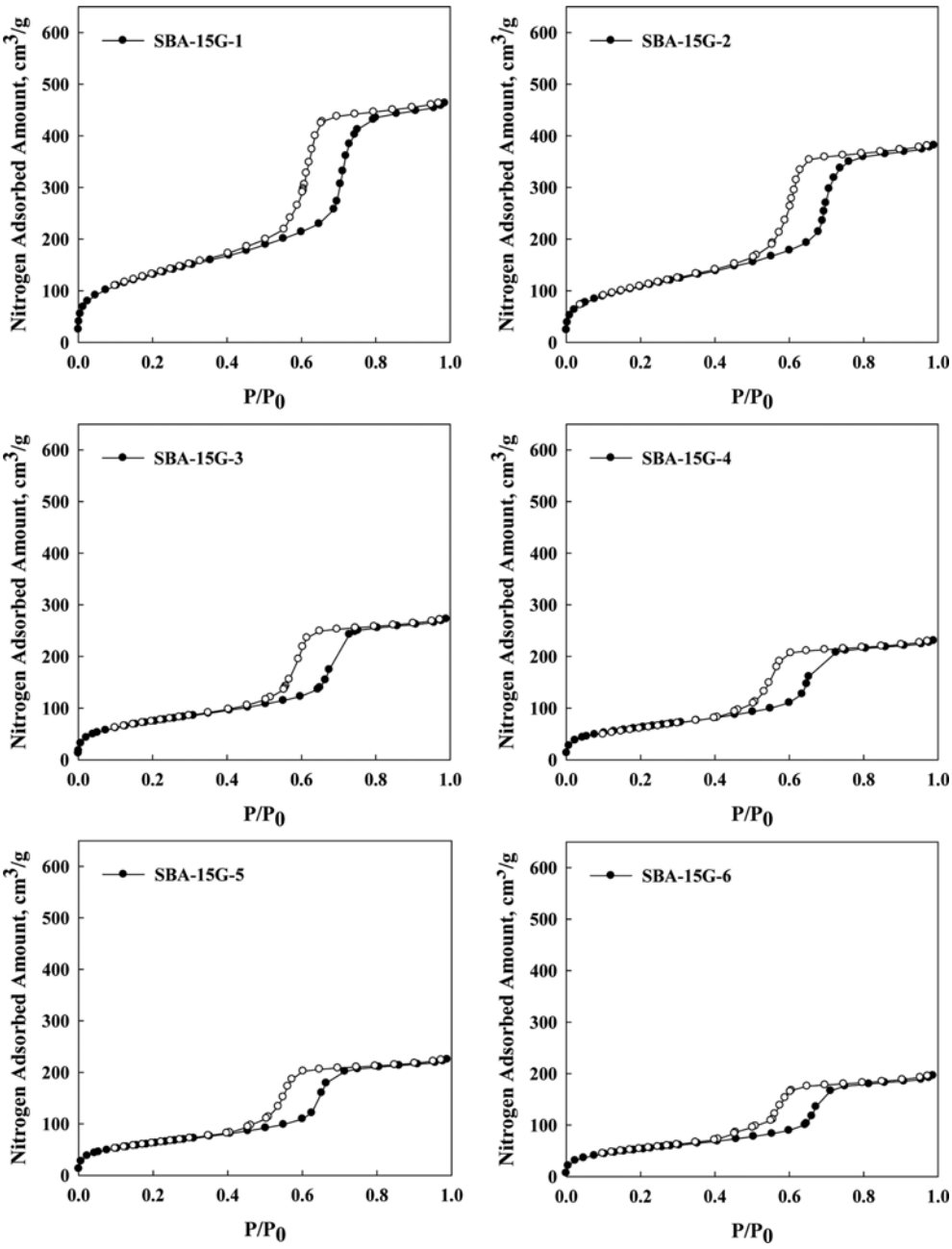

Fig. 7. Nitrogen adsorption and desorption curves for amine-grafted SBA-15G series materials.

ordered mesoporous silica, SBA-15, was successfully synthesized in the batch reactor. Figs. 3(c) and (d) of the amine-grafted and magnetized 67-SBA-15MG materials show a significant number of dots on the external surface of the mesoporous silica. However, the material maintains its 2D-hexagonal and mesoporous structure, as mentioned in the discussion on their XRD patterns above. Since the TEM images of the SBA-15G-4 material do not show any difference from those of the pristine SBA-15 material, they are not shown in this paper.

The EDS results, shown in Fig. 4, indicate that iron is well distributed on the surface of 67-SBA-15MG, as expected. In addition, Table 1 shows the weight and atomic percentages of all elements for 67-SBA-15MG, as detected by EDS. The C-K series represents the template for the sample in the TEM analysis. The Si and O series represent two main elements of the pristine mesoporous silica, SBA-15. Based on these results, it can be concluded that approximately 14 wt% of iron is distributed uniformly on the particle surfaces. Furthermore, Fig. 5 shows that the amine-grafted and magnetized SBA-15 (i.e., 67-SBA-15MG) can be completely separated from the aqueous solution within 5 min using a mag-

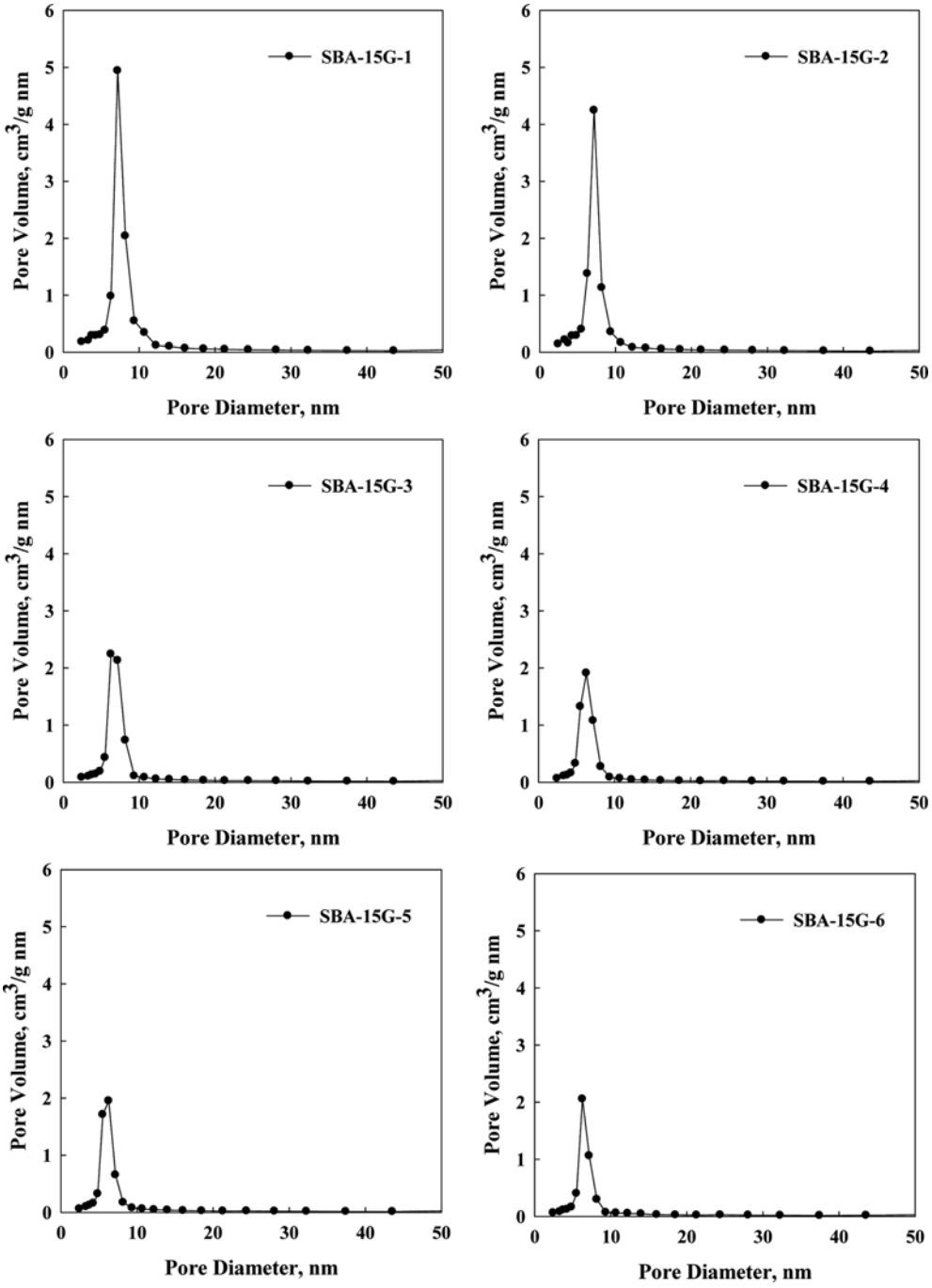

Fig. 8. BJH pore size distributions for amine-grafted SBA-15G series materials.

netic bar.

Fig. 6 shows the nitrogen adsorption/desorption data and BJH pore size distribution of the pristine SBA-15 synthesized in the batch reactor. Hysteresis is evident in Fig. 6(a). This indicates that the mesoporous structure, with a narrow pore size distribution, is well developed. The BET surface area of the prepared SBA-15 is 699 m^2/g. Furthermore, the BJH pore size distribution shows a sharp peak indicating a uniform pore size distribution. The SBA-15 has an average pore diameter of 8.19 nm and the total pore volume of 0.86 cm^3/g, as listed in Table 2. The BET surface area, and average pore size, of all the amine-grafted SBA-15G series samples, are less than those of pristine SBA-15, as shown in Figs. 7 and 8. The corresponding values are listed in Table 2 along with the total pore volume. Fig. 7 shows two typical results. First, the amount of nitrogen adsorbed at saturation pressure gradually decreases with the amount of APTES used during amine grafting. This result is expected in light of the blocking effect of the grafted amine groups on mesoporous pores. In addition, the hysteresis loop becomes small and slightly shifted to the left in terms of the relative pressure, which indicates that the pore size is also reduced with extended amine-grafting. Fig. 8 clearly shows that the pore volume (i.e., the peak height) continuously decreases, and the peak shifts slightly to the left, showing a decrease in the average pore size of the samples amine-grafted with APTES. As shown in Table 2, the BET surface area decreases from 699 to 192 m^2/g, and the average pore diameter also gradually decreases from 8.19 to 6.30 nm, after amine-grafting.

2. Effect of Amine-grafting on Adsorption of Nitrate

Fig. 9 shows the adsorption isotherms of nitrate on the amine-grafted SBA-15G series materials. We prepared six samples (SBA-15G-1~6) with different amounts of APTES used during amine-grafting, as mentioned in section 2.2. All the adsorption data give good fits to the Langmuir isotherm equation. The corresponding Langmuir parameters are listed in Table 3, with R^2 values close to unity obtained. This indicates that the Langmuir isotherm gives a satisfactory fit to the adsorption equilibrium data. The most interesting observation is that the adsorption capacity of the SBA-15G series does not always increase with the amount of APTES used during amine-grafting. When the amount of APTES is increased from 0.8 to 8.0 mmol, the nitrate adsorption capacity initially increases prior to subsequently gradually decreasing, showing a maximum at a concentration of 4.8 mmol of APTES. Looking at the isotherm parameters of the SBA-15G series samples listed in Table 3, it is evident that the SBA-15G-4 sample has the highest monolayer capacity, q_m, of 84.07 mg/g. Although this value is only an isotherm parameter, it can be used as a comparative index to show the change in adsorption capacity within a series of samples. Despite the effect of Langmuir constant, b, the optimum amount of APTES in the amine-grafting is approximately 4.8 mmol for SBA-15G series. This result is expected considering the BET results given in Table 2. The BET surface area and total pore volume are considerably reduced with increasing concentration of APTES during in amine-grafting. This implies that, although the surface area of pores is considerably reduced by grafting, the amine functional groups formed by APTES are nevertheless accessible for the adsorption of nitrate. Also, the pristine (original) SBA-15 exhibits a very low nitrate adsorption capacity compared to the amine-grafted samples [17,25]. To investigate the effect of amine-grafting more systematically, the amounts of nitrate adsorption at equilibrium, on the SBA-15G series samples, were measured with the same initial concentration of 300 mg/L (which entails that the final concentrations are different at equilibrium). The results are listed in Table 2, along with the amounts of amine attached to the samples. The amount of amine on the samples is calculated from the difference in the mass before and after amine-grafting. According to Table 2, the maximum adsorption capacity of 44.9 mg/g of nitrate is obtained as on the SBA-15G-4 sample (the SBA-15G-5 sample has the highest amine loading of 0.378 g/g). This capacity compares well with other literature reports and is much higher than that of pristine SBA-15 [25]. Hence, amine-grafting can be an effective method for enhancing the nitrate adsorption capacity of mesoporous silica materials. The decrease in the adsorption capacity when more than 4.8 mmol of APTES is used during amine-grafting can be explained by the antithetic effects of amine-grafting and blocking of silica pores. Table 2 shows that the nitrate adsorption capacity increases with the amount of amine grafted onto

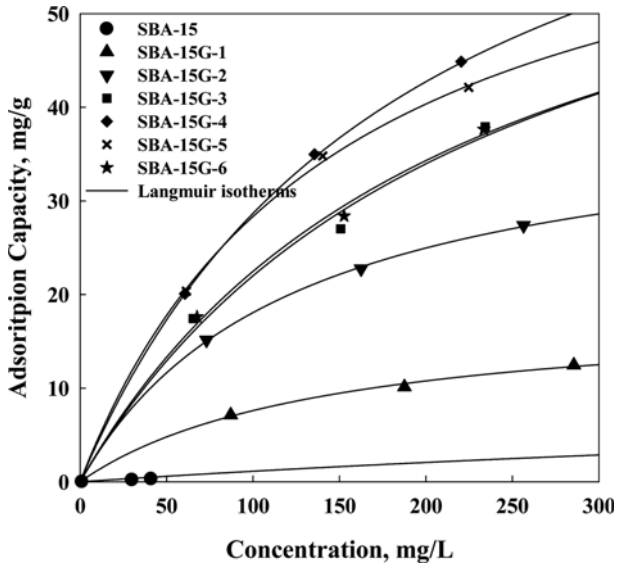

Fig. 9. Adsorption isotherms of nitrate on amine-grafted SBA-15G series materials.

Table 3. Langmuir isotherm parameters for nitrate adsorption on amine-grafted SBA-15G series materials

Adsorbents	Temperature	Langmuir isotherm		
	°C	q_m (mg/g)	b (L/mg)	R^2
SBA-15	20	12.4	0.001	0.990
SBA-15G-1		18.4	0.007	0.997
SBA-15G-2		40.38	0.008	0.999
SBA-15G-3		74.36	0.004	0.988
SBA-15G-4		84.07	0.005	0.999
SBA-15G-5		70.00	0.007	0.999
SBA-15G-6		72.42	0.005	0.996

the SBA-15 even though the BET surface area appreciably deceases with it. This clearly indicates that the adsorption of nitrate greatly depends on the amount of amine loaded onto the SBA-15, rather than on the BET surface area.

3. Effect of Magnetization

Reuse of spent adsorbents requires that the adsorbents can be recovered from the working solution and regenerated. When powder-type adsorption media are used, the introduction of magnetism is known to be especially effective for recovering spent solids [21]. However, the magnetization on the mesoporous silica materials can mask amine functional groups grafted on the silica surface. This leads to an eventual decrease in the nitrate adsorption capacity [17]. Therefore, an appropriate amount of γ-hematite must be loaded during magnetization. The adsorption isotherms of nitrate on the SBA-15MG series materials are shown in Fig. 10. Three different SBA-15MG samples were prepared by magnetization using different amounts of iron nitrate, namely 57, 67 and 73 wt% of the total weight (SBA-15+iron nitrate), and amine-grafting (the content of amine of the sample SBA-15G-5), as given in the section 2.2. Based on the weight of γ-hematite in the magnetized sample, the amounts of γ-hematite for the aforementioned samples are 34, 44 and 51 wt%, respectively. The adsorption isotherm data for the three SBA-15MG samples were fitted to the Langmuir isotherm, and the values for the parameters are listed in Table 4. As a matter of convenience, the first number in the sample names represents the weight percent of iron nitrate used in the magnetization step. In the case of 73-SBA-15MG, the nitrate adsorption capacity is 13.4 mg/g, which corresponds to approximately 32% of the nitrate adsorption capacity of the original SBA-15G-5. The high weight percent of γ-hematite results in strong magnetism for the mesoporous silica, thereby facilitating separation. However, this also results in a considerable decrease in the adsorption of nitrate. In contrast, the 57-SBA-15MG material does not have enough magnetic strength for separation; however, here the reduction in the nitrate adsorption capacity is relatively small. These results demonstrate that a γ-hematite content of between 34 and 51 wt% is required to achieve sufficient magnetic strength. Nevertheless, the 67-SBA-15MG material has sufficient magnetic strength while also exhibiting a nitrate adsorption capacity of 34.1 mg/g, which is approximately 81% of the adsorption capacity of the original SBA-15G-5 material, shown in Table 4. The results outlined above indicate that a γ-hematite content of approximately 44 wt% (of the 67-SBA-15MG) is required to guarantee both sufficient nitrate adsorption capacity and sufficient magnetic strength in the same material.

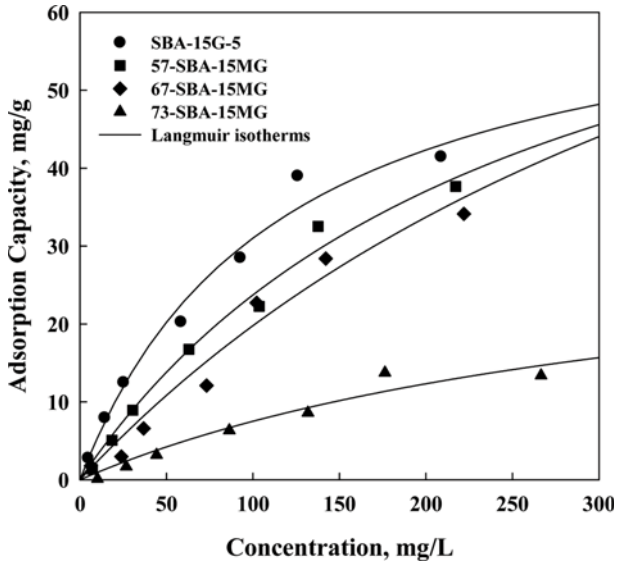

Fig. 10. Nitrate adsorption isotherms for amine-grafted and magnetized SBA-15MG series materials.

Table 4. Langmuir isotherm parameters for nitrate adsorption on amine-grafted and magnetized SBA-15MG series materials at 20 °C

Adsorbents	Iron content	Langmuir isotherm			q_e^*
	wt%	q_m (mg/g)	b (L/mg)	R^2	(mg/g)
73-SBA-15MG	51	34.3	0.003	0.936	13.4
67-SBA-15MG	44	114.0	0.002	0.960	34.1
57-SBA-15MG	34	84.5	0.004	0.983	37.7

*Adsorption amounts at equilibrium using initial concentration of 300 mg/L

A further interesting result of using the SBA-15MG series materials is the effect of γ-hematite on the nitrate adsorption capacity. As shown in Table 4, the nitrate adsorption capacity per unit mass decreases with the γ-hematite content. However, it is much higher than expected from only the weight of SBA-15M-5, under an assumption that γ-hematite does not adsorb nitrate. This demonstrates that γ-hematite has considerable nitrate adsorption capacity through adsorption [26] and catalysis [27].

4. Adsorption/Desorption Cycle Experiments

To investigate the retention of nitrate adsorption capacity and magnetic strength, adsorption/desorption experiments were carried over ten cycles. Fig. 11 shows the changes in nitrate adsorption capacity with cycle number. In all experiments, 0.1 g of new or regenerated silica material was equilibrated in a 50 ml nitrate solution with an initial nitrate concentration of 100 mg/L. The

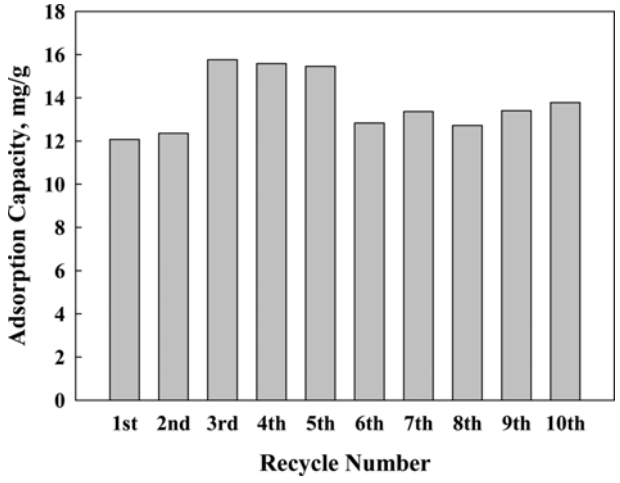

Fig. 11. Repeated nitrate adsorption on regenerated 67-SBA-15MG.

spent silica powder was treated with 0.01 M NaOH solution to desorb nitrate and reactivated with 0.1 M HCl solution to protonate the amine functional groups (-NH_2) on silica surface to -NH_3^+ for reuse. During repeated regeneration, the nitrate adsorption capacity fluctuates from 15.8 to 12.1 mg/g, as shown in Fig. 11. It increases slightly at the beginning prior to approaching to a stable value within experimental error. Even after ten cycles, the regenerated silica powder can be recovered by external magnetic force without any significant loss. The amine-grafted and magnetized SBA-15 clearly maintains its nitrate adsorption capacity, and sufficient magnetic strength for separation, after repeated adsorption-regeneration-reactivation cycles.

CONCLUSIONS

A typical mesoporous silica, SBA-15, was synthesized by hydrothermal reaction and modified by amine-grafting and magnetization to obtain a reusable powder-type adsorbent for recovering nitrate from water streams. All prepared materials were characterized by XRD, FT-IR, nitrogen adsorption/desorption, and TEM analyses to investigate their physicochemical properties. Subsequently, the materials were tested for retention of nitrate adsorption capacity and magnetic strength after repeated use.

When the ratio of SBA-15 and APTES is 10:3 (corresponding to 4.8 mmol APTES and 1 g of SBA-15) during amine-grafting, the resulting material (SBA-15G-4) exhibits the highest nitrate adsorption capacity of 44.9 mg/g. This is approximately fifteen-times than the capacity of the original pristine SBA-15 material (2.86 mg/g). In the case of amine-grafted SBA-15G series material, the nitrate adsorption capacity increases with the amount of grafted amine despite a gradual decrease in the BET surface area due to pore blocking. This suggests that the nitrate adsorption is influenced more by the amount of amine loaded on the SBA-15 than by the BET surface area.

We also determined the amount of γ-hematite required for effective magnetization of amine-grafted SBA-15G series materials. According to the experimental data, a γ-hematite content of approximately 44 wt% is required in the magnetized silica medium (corresponding to the sample 67-SBA-15MG) to guarantee both high nitrate adsorption capacity and sufficient magnetic strength for separation. In this case, the sample maintains about 81% of the nitrate adsorption capacity of the corresponding non-magnetized SBA-15G-5 material.

Furthermore, the amine-grafted and magnetized 67-SBA-15MG material maintained its adsorption capacity and magnetic strength without any noticeable loss after ten repeated adsorption-regeneration-reactivation cycles. In conclusion, the amine-grafted and magnetized mesoporous silica, SBA-15, can be used as magnetically recyclable adsorbent for recovering of nitrate from water streams. This may be employed to recover valuable nutrients and resources from wastewaters.

ACKNOWLEDGMENTS

This research was supported by the Ministry of Science, ICT and Future Planning, Republic of Korea (NRF-2013R1A1A2012668).

REFERENCES

1. S. Ghafari, M. Hasan and M. K. Aroua, *Bioresour. Technol.*, **99**, 3965 (2008).
2. M. Shrimali and K. P. Singh, *Environ. Pollut.*, **112**, 351 (2001).
3. C. Playchoom, W. Pungrasmi and S. Powtongsook, Effect of carbon sources and carbon/nitrogen ratio on nitrate removal in aquaculture denitrification tank, 2010 Int. Conf. on Biology, Environ. and Chem. IPCBEE, 1, 307, IACSIT Press, Singapore (2011).
4. J. Schick, P. Caullet, J. L. Paillaund, J. Patarin and C. M. Callarec, *Micropor. Mesopor. Mater.*, **142**, 549 (2011).
5. A. Kappor and T. Viraraghavan, *J. Environ. Eng.*, **123**, 371 (1997).
6. V. B. Jensen, J. L. Darby, C. Seidel and C. Gorman, *Crit. Rev. Env. Sci. Tec.*, **44**, 2203 (2014).
7. P. Loaganathan, S. Vigneswaran and J. Kandasamy, *J. Environ. Manage.*, **131**, 363 (2013).
8. A. Bhatnagar and M. Sillanpaa, *Chem. Eng. J.*, **168**, 493 (2011).
9. S. Chatterjee and S. H. Woo, *J. Hazard. Mater.*, **164**, 1012 (2009).
10. S. Jun, J. M. Kim, R. Ryoo, Y. S. Ahn and M. H. Han, *Micropor. Mesopor. Mater.*, **41**, 119 (2000).
11. J. S. Beck, J. C. Vartuli, W. J. Roth, M. E. Leonowicz, C. T. Kresge, K. D. Schmitt, C. T.-W. Chu, D. H. Olson, E. W. Sheppard, S. B. McCullen, J. B. Higgins and J. L. Schlenker, *J. Am. Chem. Soc.*, **114**, 10834 (1992).
12. D. Zhao, J. Feng, Q. Huo, N. Melosh, G. H. Fredrickson, B. F. Chmelka and G. D. Stucky, *Science*, **279**, 548 (1998).
13. T. P. B. Nguyen, J. W. Lee, W. G. Shim and H. Moon, *Micropor. Mesopor. Mater.*, **110**, 560 (2008).
14. M. Mesa, L. Sierra and J. L. Guth, *Micropor. Mesopor. Mater.*, **112**, 338 (2008).
15. M. Kruk, M. Jaroniec, C. H. Ko and R. Ryoo, *Chem. Mater.*, **12**, 1961 (2000).
16. Y. Kim, J. Bae, J. Park, J. Suh, S. Lee, H. Park and H. Choi, *Chem. Eng. J.*, **256**, 475 (2014).
17. R. Saad, S. Hamoudi and K. Belkacemi, *J. Porous Mater.*, **15**, 315 (2008).
18. E. Dana, N. D. Silva and A. Sayari, *Chem. Eng. J.*, **166**, 454 (2011).
19. A. Benhamou, J. P. Basly, M. Baudu, Z. Derriche and R. Hamacha, *J. Colloid Interface Sci.*, **404**, 135 (2013).
20. T. Yokoi, H. Yoshitake, T. Yamada, Y. Kubota and T. Tatsumi, *J. Mater. Chem.*, **16**, 1125 (2006).
21. B. C. Kim, J. Lee, W. Um, J. Kim, J. Joo, J. H. Lee, J. H. Kwak, J. H. Kim, C. Lee, H. Lee, R. S. Addleman, T. Hyeon, M. B. Gu and J. Kim, *J. Hazard. Mater.*, **192**, 1140 (2011).
22. J. Lee, H. B. Na, B. C. Kim, J. H. Lee, B. Lee, J. H. Kwak, Y. Hwang, J. G. Park, M. B. Gu, J. Kim, J. Joo, C. H. Shin, J. W. Grate, T. Hyeon and J. Kim, *J. Mater. Chem.*, **19**, 7864 (2009).
23. A. B. Bourlinos, A. Simopoulos, N. Boukos and D. Petridis, *J. Phys. Chem. B*, **105**, 7432 (2001).
24. K. Bachari and A. Touileb, *Solid State Sci.*, **11**, 1549 (2009).
25. J. Y. Kim, M. S. Balathanigaimani and H. Moon, *Water Air Soil Poll.*, **226**, 431 (2015).
26. E. A. Zorgani, A. Cibati and C. Trois, *Water Air Soil Poll.*, **227**, 249 (2016).
27. G. C. C. Yang and H. L. Lee, *Water Res.*, **39**, 884 (2005).